Growth index and statefinder diagnostic of oscillating dark energy

Grigoris Panotopoulos*
Centro de Astrofísica e Gravitação, Instituto Superior Técnico-IST, Universidade de Lisboa-UL, Av. Rovisco Pais, 1049-001 Lisboa, Portugal

Ángel Rincón†
Instituto de Física, Pontificia Universidad Católica de Chile, Avenida Vicuña Mackenna 4860, Santiago, Chile

(Received 29 January 2018; published 16 May 2018)

We study in some detail the cosmology of oscillating dark energy described by concrete equations-of-state introduced recently in the literature. In particular, we compute the statefinder parameters, the growth index, as well as the combination parameter $A = f\sigma_8$, and a comparison with the concordance ΛCDM is made.

DOI: 10.1103/PhysRevD.97.103509

I. INTRODUCTION

At the end of the 1990s, the breakthrough in science was the discovery that the Universe is expanding at an accelerating rate [1,2]. More recent well-established observational data coming both from cosmology and sstrophysics indicate that our observed Universe is spatially flat and dominated by dark energy [3], the origin and nature of which remain a mystery. The concordance cosmological model, based on cold dark matter and a cosmological constant (or ΛCDM model), which can be viewed as a perfect fluid with a constant equation of state $w = -1$, is the most economical one in excellent agreement with current data. Despite its success, it suffers from the cosmological constant problem [4]. Therefore, other possibilities have been explored in the literature over the years, which in general fall into broad classes, namely either dynamical or geometrical models of dark energy. In the first class, a new field is introduced to accelerate the Universe [5], while in the second one an alternative theory of gravity is assumed to modify Einstein's general relativity at cosmological scales [6–8].

Although a model derived from a Lagrangian description is clearly preferred, in practice a phenomenological description, in which dark energy is viewed as a perfect fluid with a time varying equation of state $w(a)$, with a being the scale factor, is simpler to study. In the past in [9], the authors compared several dark energy parametrizations to supernovae data, and concluded that models that cross the $w = -1$ barrier have a better fit to data. In addition, more recently it was shown that the cosmic acceleration may have slowed down recently [10]. Oscillating Dark Energy (ODE) is a class of dark energy parametrization that has been studied by several authors and in different contexts [11–16], and very recently in [17], during the last 15 years or so. A couple of reasons why studying this particular class of models is interesting are the following: In [11], it was demonstrated that ODE may alleviate the coincidence problem, while in [13] it was shown that unifying the current cosmic acceleration with the inflationary Universe was possible. One of the first papers along these lines was the work of [12], in which the graceful exit of cosmological inflation and reheating of the Universe were studied in the framework of dynamical relaxation of a bare cosmological constant.

It is well known that the predictions of many dark energy models are consistent with the available data, since they predict very similar expansion histories. It thus becomes clear that, in order to discriminate between different dark energy models, it is important to introduce and study new quantities appropriately defined. To this end one option would be to study the so-called statefinder parameters, r, s, defined as follows [18,19]

$$r = \frac{\dddot{a}}{aH^3} \tag{1}$$

$$s = \frac{r-1}{3(q-\frac{1}{2})} \tag{2}$$

where the dot denotes differentiation with respect to the cosmic time, $H = \dot{a}/a$ is the Hubble parameter, and $q = -\ddot{a}/(aH^2)$ is the decelerating parameter. Contrary to the Hubble parameter and the decelerating parameter, that are expressed in terms of the first and the second time

*grigorios.panotopoulos@tecnico.ulisboa.pt
†arrincon@uc.cl

derivative of the scale factor, respectively, the statefinder parameters are expressed in terms of the third derivative of the scale factor a with respect to the cosmic time t. These parameters may be computed within a certain model, their values can be extracted from future observations [20,21], and as we will show later on can be very different from one model to another even if the expansion histories are very similar to one another. It is easy to check that for the ΛCDM model the statefinder parameters are just constants, $r = 1$, $s = 0$. The statefinder diagnostics has been applied to several dark energy models [22–26].

A second option would be to investigate how matter perturbations evolve, as its evolution is sensitive to the sound speed of dark energy, that differs from one model to another. In particular, a quantity that has been studied a lot over the years is the so called growth index γ, introduced in [27] and to be defined later on, and for the ΛCDM model has been found to be $\gamma_{\Lambda\mathrm{CDM}} = 6/11 \simeq 0.55$ [28–30].

It is the goal of the present article to further study the cosmology of the oscillating dark energy models introduced recently [17] in more detail along the lines mentioned before. Our work is organized as follows: after this introduction, we present the theoretical framework in the second section, and we present our numerical results in Sec. III. Finally we conclude in the last section.

II. THEORETICAL FRAMEWORK

Here we introduce all the necessary ingredients, first for the background evolution and then for the evolution of cosmological perturbations.

A. Background evolution

The time dependence of the scale factor is determined by the first and the second Friedmann equations of a flat Robertson-Walker metric

$$H^2 = \frac{8\pi G\rho}{3} \tag{3}$$

$$\dot{H} = -4\pi G(\rho + p) \tag{4}$$

where G is Newton's constant, $\rho = \rho_m + \rho_r + \rho_X$ is the total energy density, $p = p_m + p_r + p_X$ is the total pressure, and the index m, r, X denotes the fluid component of matter, radiation, and dark energy, respectively. It is convenient to define the normalized energy density for each fluid, $\Omega_A \equiv \rho_A/\rho$ to be used later on, and the condition $\sum_A \Omega_A \equiv 1$ has to be satisfied. What is more, assuming no interaction between the fluid components, the continuity equation for each fluid reads

$$\dot{\rho_A} + 3H\rho_A(1 + w_A) = 0 \tag{5}$$

where the index A takes 3 values, $A = m$, r, X. The equation-of-state parameter for matter is $w_m = 0$, for radiation $w_r = 1/3$, while for dark energy we shall assume some parametrization where its equation of state will be a certain function of the redshift $1 + z = a_0/a$, with a_0 being today's value of the scale factor a.

The cosmological equations together with the definitions allow us to compute both the deceleration parameter q and the first statefinder parameter r as functions of the redshift, which are found to be

$$q(z) = -1 + (1 + z)\frac{E'(z)}{E(z)} \tag{6}$$

$$r(z) = q(z)(2q(z) + 1) + (1 + z)q'(z) \tag{7}$$

while the second statefinder parameter s can be computed accordingly using its definition. The prime denotes differentiation with respect to redshift, and $E(z) = H(z)/H_0$ is the dimensionless Hubble parameter versus redshift, with $H_0 = 100\ h(\mathrm{km\,sec}^{-1})/\mathrm{Mpc}$ being the Hubble constant. It is easy to verify that the expressions above in the case of the ΛCDM model give $r = 1$, $s = 0$. For matter and radiation, the normalized energy densities are given by

$$\Omega_m(z) = \frac{\Omega_{m,0}(1 + z)^3}{E(z)^2} \tag{8}$$

$$\Omega_r(z) = \frac{\Omega_{r,0}(1 + z)^4}{E(z)^2} \tag{9}$$

where $\Omega_{m,0}$, $\Omega_{r,0}$ are today's values of the normalized densities for matter and radiation, respectively. Finally, for a given dark energy parametrization $w(z)$, the dimensionless Hubble parameter $E(z) = H(z)/H_0$ is given by

$$E(z) = \sqrt{\Omega_{m,0}(1 + z)^3 + \Omega_{r,0}(1 + z)^4 + (1 - \Omega_{m,0} - \Omega_{r,0})F(z)} \tag{10}$$

where $\Omega_{r,0} = 9 \times 10^{-5}$ [10], and where the function $F(z)$ is computed once the dark energy equation of state is given [9]

$$F(z) = \exp\left(3\int_0^z dx\frac{1 + w(x)}{1 + x}\right) \tag{11}$$

We see that $F(0) = 1 = E(0)$, as they should, since the condition $\sum_A \Omega_A \equiv 1$ should be always satisfied, as we have already mentioned.

B. Cosmological perturbations

Now we move on to discuss linear cosmological perturbation theory [31–34]. Only scalar perturbations are relevant to structure formation, and assuming vanishing anisotropic stress tensor for the fluid components, the metric is characterized by a single Bardeen potential $\Psi(\eta, \vec{x})$

$$ds^2 = a(\eta)^2[-(1+2\Psi)d\eta^2 + (1-2\Psi)\delta_{ij}dx^i dx^j] \tag{12}$$

with $d\eta = dt/a$ being the conformal time. On the one hand, the differential equations for the metric perturbation are derived from the perturbed Einstein's equations $\delta G_{\mu\nu} = 8\pi G \delta T_{\mu\nu}$, which in Fourier space take the form [33]

$$3\mathcal{H}(\mathcal{H}\Psi + \Psi') + k^2\Psi = -4\pi G a^2 \delta\rho \tag{13}$$

$$\mathcal{H}\Psi + \Psi' = -4\pi G a^2 (\rho + p) v \tag{14}$$

$$\Psi'' + 3\mathcal{H}\Psi' + \Psi(\mathcal{H}^2 + 2\mathcal{H}') = 4\pi G a^2 \delta p \tag{15}$$

where $\delta p = \sum_A \delta p_A$ is the total pressure perturbation, $\delta\rho = \sum_A \delta\rho_A$ is the total energy density perturbation, and $(1+w)v = \sum_A (1+w_A)\Omega_A v_A$ is the total peculiar velocity potential [33]. On the other hand, the stress tensor conservation for each fluid provides us with additional differential equations for the peculiar velocity potential v and density contrast $\delta_A = \delta\rho_A/\rho_A$. Defining the total density contrast $\delta = \delta\rho/\rho = \sum_A \Omega_A \delta_A$, and using as independent variable $x = -\ln(1+z)$, so that for any variable $A' = \mathcal{H}A_x$, we finally obtain the following equations for the metric perturbation [33]

$$\Psi_x + \Psi\left(1 + \frac{k^2}{3\mathcal{H}^2}\right) = -\frac{\delta}{2} \tag{16}$$

$$\Psi_x + \Psi = -\frac{3}{2}\mathcal{H}v(1+w) \tag{17}$$

as well as the following equations, both for δ and v, for all three fluid components [33]

$$(\delta_r)_x = \frac{4}{3}\left(3\Psi_x + v_r \frac{k^2}{\mathcal{H}}\right) \tag{18}$$

$$(v_r)_x = -\frac{1}{\mathcal{H}}\left(\Psi + \frac{\delta_r}{4}\right) \tag{19}$$

$$(\delta_m)_x = 3\Psi_x + v_m \frac{k^2}{\mathcal{H}} \tag{20}$$

$$(v_m)_x = -\left(v_m + \frac{\Psi}{\mathcal{H}}\right) \tag{21}$$

$$(\delta_X)_x = 3(w_X - c_{X,s}^2)\delta_X + (1+w_X) \times \left[3\Psi_x + v_X\left(\frac{k^2}{\mathcal{H}} + 9\mathcal{H}(c_{X,s}^2 - c_{X,a}^2)\right)\right] \tag{22}$$

$$(v_X)_x = v_X(3c_{X,s}^2 - 1) - \frac{1}{\mathcal{H}}\left(\Psi + \delta_X \frac{c_{X,s}^2}{1+w_X}\right) \tag{23}$$

where the adiabatic speed of sound $c_{A,a}^2$ is defined by [32,33]

$$c_{A,a}^2 = \frac{\dot{p_A}}{\dot{\rho_A}} = w_A - \frac{\dot{w_A}}{3H(1+w_A)} \tag{24}$$

while the effective speed of sound in the rest frame of the fluid $c_{A,s}^2$ is defined by [32,33]

$$\delta p_A = c_{A,s}^2 \delta\rho_A - 3\mathcal{H}(1+w_A)\rho_A v_A (c_{A,s}^2 - c_{A,a}^2) \tag{25}$$

with $\mathcal{H}a = da/d\eta$ being the conformal Hubble parameter, and the prime denotes differentiation with respect to the conformal time. The speeds of sound are found to be $c_{m,a}^2 = 0 = c_{m,s}^2$ for matter, $c_{r,a}^2 = 1/3 = c_{r,s}^2$ for radiation, while for dark energy, following [17], we have taken $c_{X,s}^2 = 1$.

Finally, the above differential equations must be supplemented with the appropriate initial conditions. Assuming adiabatic initial conditions for any two fluids i, j

$$\frac{\delta_i}{1+w_i} = \frac{\delta_j}{1+w_j} \tag{26}$$

one obtains the following initial conditions for the peculiar velocity potentials [33]

$$v_{A,\mathrm{ini}} = \frac{\delta_{\mathrm{ini}}}{4\mathcal{H}_{\mathrm{ini}}} \tag{27}$$

while for the density contrasts we obtain

$$\delta_{A,\mathrm{ini}} = \frac{3}{4}(1 + w_{A,\mathrm{ini}})\delta_{\mathrm{ini}} \tag{28}$$

starting from the radiation dominated era where $z_{\mathrm{ini}} = 10^6$ or $x_{\mathrm{ini}} = -13.81$. For the Hubble constant H_0, we have used the results of [17] shown in Tables II, III, and IV of that work.

The growth index γ is defined through the relation below [35–37], and for more recent discussions, see e.g. [38–41]

$$\frac{d(\ln\delta_m)}{d(\ln a)} = f = \Omega_m^\gamma \tag{29}$$

Therefore, after integrating the full system of equations, first we compute the function f from the matter energy density contrast, and then the growth index can be computed by

$$\gamma = \frac{\ln(f)}{\ln(\Omega_m)} \tag{30}$$

Note that we could have integrated the equations for the perturbations using one of the publicly available computer codes, such as CMBFAST [42] or CAMB [43] or CMB-easy [44,45]. However, since here we are not interested in the temperature anisotropies, we have opted to integrate the equations numerically using a MATHEMATICA [46] file as was done in [47].

III. NUMERICAL RESULTS

We can now analyse any dark energy model with a given parametrization $w(z)$. Here we analyse the following 3 oscillatory equation-of-state parameters introduced recently in the literature by the authors of [17]

$$w_I(z) = w_0 + b[1 - \cos[\ln(1+z)]] \tag{31}$$

$$w_{II}(z) = w_0 + b\sin[\ln(1+z)] \tag{32}$$

$$w_{III}(z) = w_0 + b\left[\frac{\sin(1+z)}{1+z} - \sin 1\right] \tag{33}$$

where $w_0 = w(0)$ is their today's value. For these parametrizations, the function $F(z)$ that determines the dimensionless Hubble parameter is found to be

$$F(z) = (1+z)^{3(1+b+w_0)} e^{-3b\sin(\ln(1+z))} \tag{34}$$

for the first model,

$$F(z) = (1+z)^{3(1+w_0)} e^{3b(1-\cos\ln(1+z))} \tag{35}$$

for the second model, and

TABLE I. Parameters involved in each model.

Parameters	Model #1	Model #2	Model #3
w_0	−1.0267	−1.0517	−1.0079
b	−0.2601	0.0113	0.1542
$\Omega_{m,0}$	0.298	0.297	0.301
H_0	68.95	69.02	68.59
σ_8	0.824	0.823	0.821

$$F(z) = F_0^b e^{3b[\mathrm{Ci}(1+z) - \frac{\sin(1+z)}{(1+z)}]}(1+z)^{3(1+w_0-b\sin(1))} \tag{36}$$

for the third model, where the cosintegral function is defined as follows:

$$\mathrm{Ci}(z) \equiv -\int_z^\infty \mathrm{d}t\,\frac{\cos(t)}{t}, \tag{37}$$

and we have introduced the real parameter $F_0 = e^{3(\sin(1) - \mathrm{Ci}(1))}$.

Using several observational data, such as supernovae type Ia, BAO distance measurements, weak gravitational lensing, CMB observations etc, the authors of [17] found the values shown in Table I.

The equation of state and the deceleration parameter versus redshift are shown in Fig. 1 for all three models. We see that (a) the equation-of-state in all three cases always remains in the range below the −1 barrier, and (b) all models predict the same decelerating parameter as a function of redshift. The first and second statefinder parameters r and s versus redshift are shown in Fig. 2 for all three models. We see that the second statefinder parameter at low redshift approaches that of ΛCDM, while at large ΛCDM deviates significantly from the standard behaviour. The opposite holds for the first parameter.

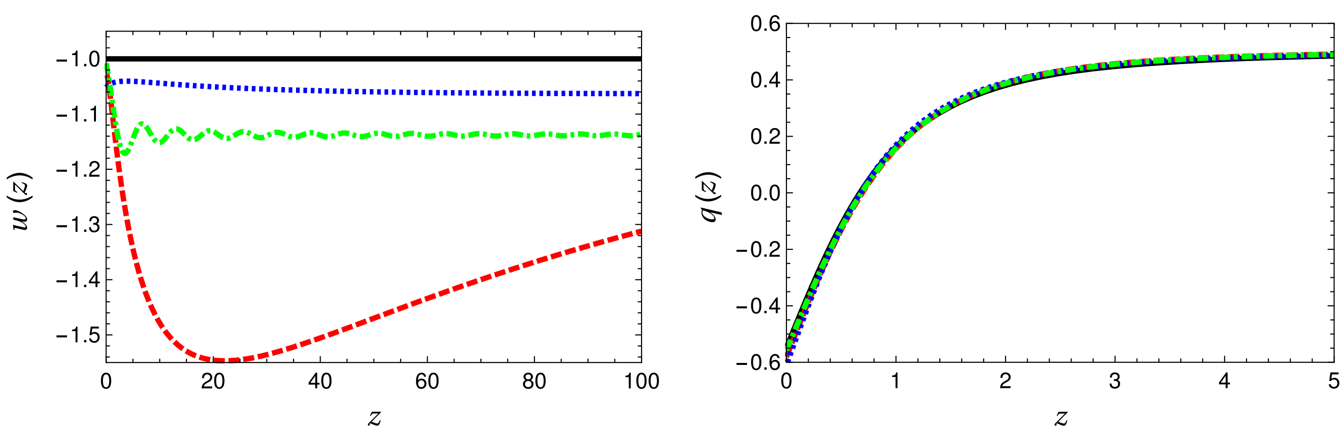

FIG. 1. *Left panel:* Equation of state parameter versus redshift for the ΛCDM model (solid black line), for the first model (dashed red line), for the second model (dotted blue line) and for the third model (dotted dashed green line). *Right panel:* Deceleration parameter q versus redshift for the ΛCDM model (solid black line), for the first model (dashed red line), for the second model (dotted blue line) and for the third model (dotted dashed green line).

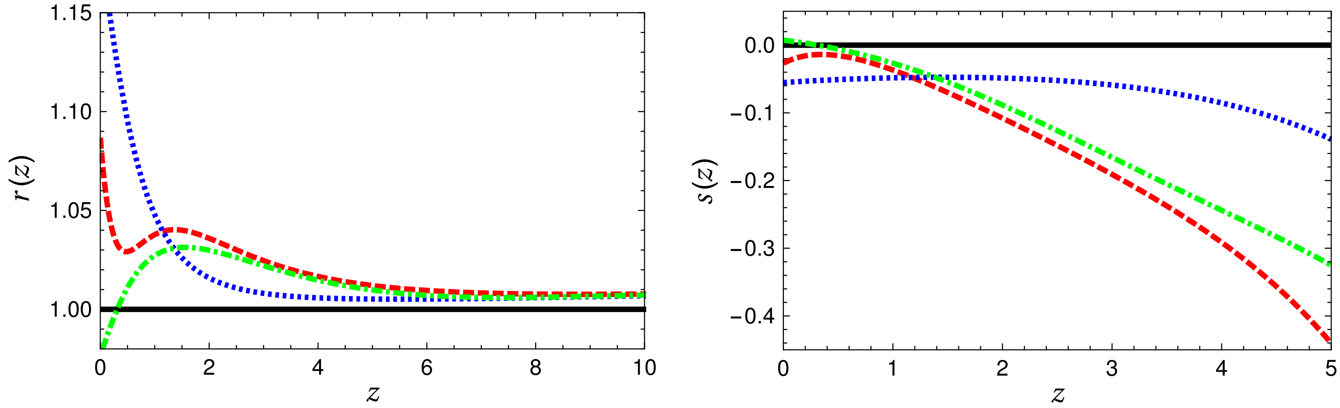

FIG. 2. *Left panel:* The first statefinder parameter r versus redshift for the ΛCDM model (solid black line), for the first model (dashed red line), for the second model (dotted blue line) and for the third model (dotted dashed green line). *Right panel:* The second statefinder parameter s versus redshift for the ΛCDM model (solid black line), for the first model (dashed red line), for the second model (dotted blue line) and for the third model (dotted dashed green line).

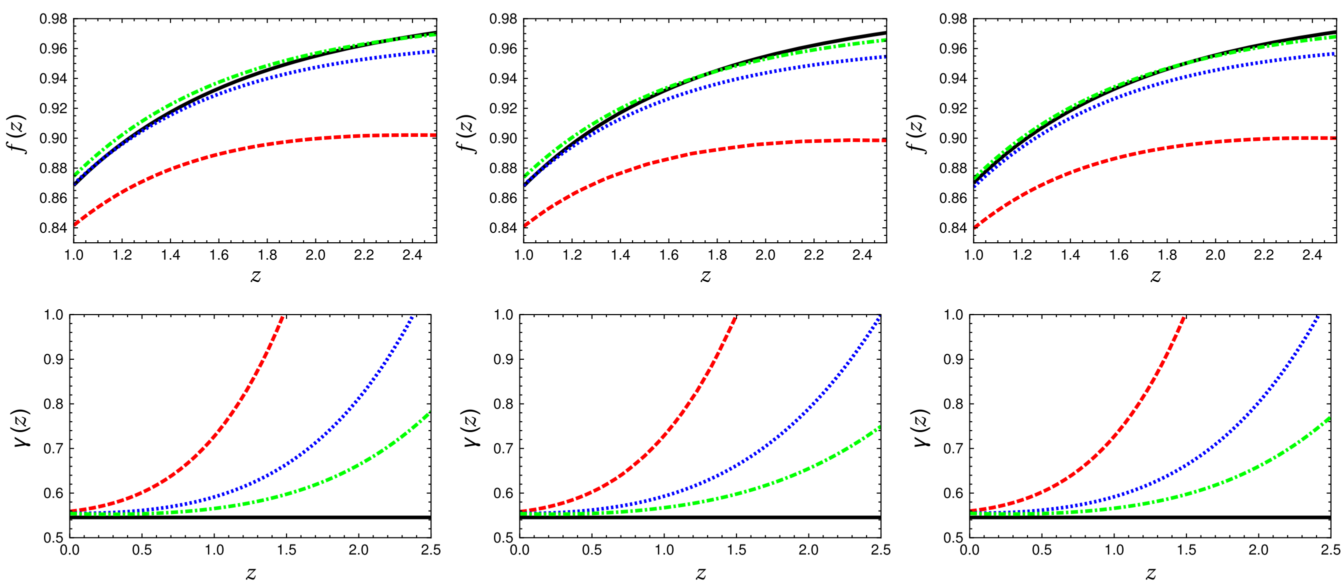

FIG. 3. The evolution of functions f and γ versus redshift z for the three models. The panels in the first (left), second (center) and third (right) column describe the functions $\{f(z), \gamma(z)\}$ for the models I, II, and III, respectively. We show the ΛCDM model (solid black line) and three different cases: (i) $k = 2 \times 10^{-3}$ h Mpc^{-1} (dashed red line), (ii) $k = 4 \times 10^{-3}$ h Mpc^{-1} (dotted blue line) and (iii) for $k = 6 \times 10^{-3}$ h Mpc^{-1} (dotted dashed green line).

Next we consider linear cosmological perturbations and the evolution of the functions $\{f(z), \gamma(z)\}$. We show the solution for the three cases studied in Fig. 3 for three different scales k of the linear regime, of the order of 10^{-3} Mpc. For comparison, we show in the same plot (solid black curves) the corresponding quantities of the ΛCDM model. We see that (i) in all three models, both f and γ increase with redshift, and (ii) as the wave number k increases, the curves approach the curve corresponding to ΛCDM.

Finally, in Fig. 4, we compare the prediction of the models to available data regarding the combination parameter $A(z) = \sigma_8(z) f(z)$, where the rms fluctuation $\sigma_8(z)$ is related to the matter energy density contrast by [28,33]

$$\sigma_8(z) = \frac{\delta_m(z)}{\delta_m(0)} \sigma_8(z = 0) \tag{38}$$

evaluated at the scale $k_{\sigma_8} = 0.125$ h Mpc^{-1} [33]. We have used for $\sigma_8(z = 0)$ the values shown in Table I obtained in [17]. The data points with the error bars as well as the relevant references can be seen in Table II of [33]. Figure 4 looks very similar to analogous figures produced in other related works, such as [33,48,49].

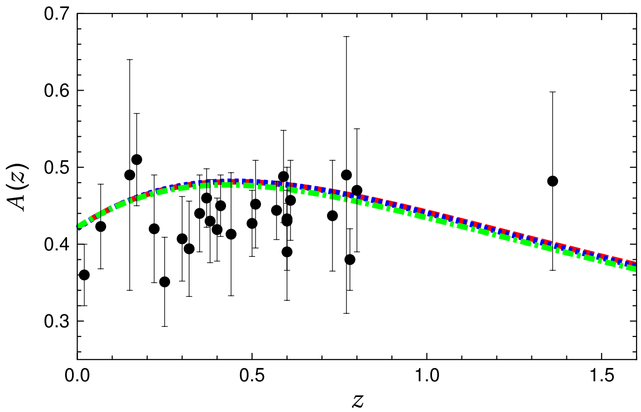

FIG. 4. Comparison between observational data (the error bars are shown too) and the prediction of the models I, II, and III for $A(z) = \sigma_8(z) f(z)$ versus redshift for $k = 125 \times 10^{-3}\,\mathrm{h\,Mpc}^{-1}$. We show the ΛCDM model (solid black line) and three different cases: (i) model I (dashed red line), (ii) model II (dotted blue line), and (iii) model III (dotted dashed green line).

IV. CONCLUSIONS

To summarize, in the present article, we have analysed in some detail the cosmology of three oscillating dark energy models, both at the level of background evolution and at the level of linear perturbations. The dark energy equations of state were recently introduced in the literature, and the free parameters of each model were determined upon comparison against several observational data. At the level of background evolution, we have computed the statefinder parameters r, s versus redshift, while at the level of linear cosmological perturbation theory, we have computed $f = (a/\delta_m) d\delta_m/da$ as well as the growth index $\gamma = \ln(f)/\ln(\Omega_m)$ as functions of the redshift for all three dark energy parametrizations and for different scales k. We have produced several plots in which our main numerical results are shown, and the comparison with the ΛCDM model is made.

ACKNOWLEDGMENTS

We wish to thank the anonymous reviewer for his/her comments and suggestions. The work of A. R. was supported by the CONICYT-PCHA/Doctorado Nacional/2015-21151658. G. P. thanks the Fundação para a Ciência e Tecnologia (FCT), Portugal, for the financial support to the Center for Astrophysics and Gravitation-CENTRA, Instituto Superior Técnico, Universidade de Lisboa, through Grant No. UID/FIS/00099/2013.

[1] A. G. Riess *et al.*, Astron. J. **116**, 1009 (1998).
[2] S. Perlmutter *et al.*, Astrophys. J. **517**, 565 (1999).
[3] W. L. Freedman and M. S. Turner, Rev. Mod. Phys. **75**, 1433 (2003).
[4] S. Weinberg, Rev. Mod. Phys. **61**, 1 (1989).
[5] E. J. Copeland, M. Sami, and S. Tsujikawa, Int. J. Mod. Phys. D **15**, 1753 (2006).
[6] G. R. Dvali, G. Gabadadze, and M. Porrati, Phys. Lett. B **485**, 208 (2000).
[7] W. Hu and I. Sawicki, Phys. Rev. D **76**, 064004 (2007).
[8] A. A. Starobinsky, JETP Lett. **86**, 157 (2007).
[9] S. Nesseris and L. Perivolaropoulos, Phys. Rev. D **70**, 043531 (2004).
[10] J. Magaña, V. H. Cárdenas, and V. Motta, J. Cosmol. Astropart. Phys. 10 (2014) 017.
[11] S. Dodelson, M. Kaplinghat, and E. Stewart, Phys. Rev. Lett. **85**, 5276 (2000).
[12] R. Brandenberger and A. Mazumdar, J. Cosmol. Astropart. Phys. 08 (2004) 015.
[13] B. Feng, M. Li, Y. S. Piao, and X. Zhang, Phys. Lett. B **634**, 101 (2006).
[14] J. Q. Xia, B. Feng, and X. M. Zhang, Mod. Phys. Lett. A **20**, 2409 (2005).
[15] D. Jain, A. Dev, and J. S. Alcaniz, Phys. Lett. B **656**, 15 (2007).
[16] R. Lazkoz, V. Salzano, and I. Sendra, Phys. Lett. B **694**, 198 (2010).
[17] S. Pan, E. N. Saridakis, and W. Yang, arXiv:1712.05746.
[18] V. Sahni, T. D. Saini, A. A. Starobinsky, and U. Alam, Pis'ma Zh. Eksp. Teor. Fiz. **77**, 249 (2003) [JETP Lett. **77**, 201 (2003)].
[19] U. Alam, V. Sahni, T. D. Saini, and A. A. Starobinsky, Mon. Not. R. Astron. Soc. **344**, 1057 (2003).
[20] J. Albert *et al.* (SNAP Collaboration), arXiv:astro-ph/0507458.
[21] J. Albert *et al.* (SNAP Collaboration), arXiv:astro-ph/0507459.
[22] W. Zimdahl and D. Pavon, Gen. Relativ. Gravit. **36**, 1483 (2004).
[23] X. Zhang, Phys. Lett. B **611**, 1 (2005).
[24] P. x. Wu and H. w. Yu, Int. J. Mod. Phys. D **14**, 1873 (2005).
[25] B. Chang, H. Liu, L. Xu, and C. Zhang, Mod. Phys. Lett. A **23**, 269 (2008).
[26] G. Panotopoulos, Nucl. Phys. **B796**, 66 (2008).
[27] L. M. Wang and P. J. Steinhardt, Astrophys. J. **508**, 483 (1998).
[28] S. Nesseris and L. Perivolaropoulos, Phys. Rev. D **77**, 023504 (2008).
[29] A. B. belloso, J. Garcia-Bellido, and D. Sapone, J. Cosmol. Astropart. Phys. 10 (2011) 010.

[30] R. C. Batista, Phys. Rev. D **89**, 123508 (2014).
[31] V. Mukhanov, *Physical Foundations of Cosmology* (Cambridge University Press, Cambridge, England, 2005).
[32] R. de Putter, D. Huterer, and E. V. Linder, Phys. Rev. D **81**, 103513 (2010).
[33] I. Albarran, M. Bouhmadi-Lpez, and J. Morais, Phys. Dark Universe **16**, 94 (2017).
[34] G. Panotopoulos, Phys. Rev. D **96**, 023520 (2017).
[35] E. V. Linder, Phys. Rev. D **72**, 043529 (2005).
[36] D. Huterer and E. V. Linder, Phys. Rev. D **75**, 023519 (2007).
[37] E. V. Linder and R. N. Cahn, Astropart. Phys. **28**, 481 (2007).
[38] G. Ballesteros and A. Riotto, Phys. Lett. B **668**, 171 (2008).
[39] J. Dossett, M. Ishak, J. Moldenhauer, Y. Gong, A. Wang, and Y. Gong, J. Cosmol. Astropart. Phys. 04 (2010) 022.
[40] S. Nesseris and D. Sapone, Phys. Rev. D **92**, 023013 (2015).
[41] S. Tsujikawa, A. De Felice, and J. Alcaniz, J. Cosmol. Astropart. Phys. 01 (2013) 030.
[42] U. Seljak and M. Zaldarriaga, Astrophys. J. **469**, 437 (1996).
[43] A. Lewis, A. Challinor, and A. Lasenby, Astrophys. J. **538**, 473 (2000).
[44] M. Doran, J. Cosmol. Astropart. Phys. 10 (2005) 011.
[45] M. Doran and C. M. Mueller, J. Cosmol. Astropart. Phys. 09 (2004) 003.
[46] Wolfram Mathematica, http://www.wolfram.com.
[47] J. C. B. Sanchez and L. Perivolaropoulos, Phys. Rev. D **81**, 103505 (2010).
[48] S. Tsujikawa, A. De Felice, and J. Alcaniz, J. Cosmol. Astropart. Phys. 01 (2013) 030.
[49] S. Basilakos, Mon. Not. R. Astron. Soc. **449**, 2151 (2015).